Influence of Crystallographic Orientation on the Mechanical Properties and Deformation Behavior of Ni Nanowire Using Large Scale Molecular Dynamics

Krishna Chaitanya Katakam, Sudhakar Rao Gorja, and Natraj Yedla

Abstract The influence of crystallographic orientation on nickel nanowire mechanical properties and deformation behavior has been studied using large-scale molecular dynamic simulations. In the model preparation, the embedded atomic method potential is used. The crystallographic orientations of Ni nanowire are [1–10], [20–1] [111] and [1–1–2]. All the tensile tests are carried at 10 K temperature and a deformation rate of 10^8 s^{-1}. The size of the Ni nanowire used for tensile studies is 100 Å (x-axis) × 1000 Å (y-axis) × 100 Å (z-axis) and comprises of ~ 925,000 atoms. The simulated results show that orientation has a significant effect on mechanical properties. Nanowire of various orientations yields by Shockley partial dislocation with intrinsic stacking faults followed by twinning partials. The yield stress of [1–20], [20–1], [111] and [1–1–2] orientations are 9.5 GPa, 11.7 GPa, 17.2 GPa and 10.5 GPa respectively.

Keywords Molecular dynamics · Nanowire · Orientation and mechanical properties

1 Introduction

In the last two decades, nanowires (NWs) importance in nanoscale electronic and mechanical systems is increasing drastically due to their application as interconnectors [1]. Nanowire one-dimensional structure and enthralling properties have made the researchers go much depth into their mechanical and physical properties for new findings during different loading conditions. Scientific interest among researchers on nanowires is mainly due to their unique performance in numerous applications [2]. Majorly in the modern functional systems like NW transistors of high mobility

K. C. Katakam (✉) · N. Yedla
Computational Materials Engineering Group, Department of Metallurgical and Materials Engineering, National Institute of Technology Rourkela, Rourkela 769008, India

S. R. Gorja
Corrosion Group, Materials Engineering Division, National Metallurgical Laboratory, Jamshedpur 831007, India

S. Pal et al. (eds.), *Processing and Characterization of Materials*, Springer Proceedings in Materials 13, https://doi.org/10.1007/978-981-16-3937-1_8

and strain-controlled logic gates, supercapacitors, conductors, and other magnetic field devices [3]. Nickel (Ni) NW is essential and widely used in electromagnetic systems, owing to its broad applications [4]. The NW applications in modern nanodevices are increasing gradually. For better functionality of these devices, it is necessary to understand the influence of crystallographic orientation, sample size, and shape on the NW deformation mechanisms and their mechanical properties.

In the last two decades, many researchers have worked experimentally and computationally in the investigation of understanding the deformation behavior of metal NWs. Many researchers have reported the size, shape, and orientation influence on the deformation mechanism of NWs [5–11]. The deformation mechanism in FCC metal NW is either by slip through partial dislocations or by twinning. NW crystallographic orientation and its loading direction mainly determine the deformation mechanism. Hence the crystallographic orientation plays a vital role, followed by loading direction in the deformation behavior of metal NWs. For instance, using molecular dynamics (MD) simulation, Park et al. [5] investigated the tensile and compressive behavior of FCC NWs (Copper, Nickel, and Gold) of <100> and <110> orientations. They said that the NW deformation mechanism depends on material intrinsic properties, crystallographic orientation, applied stress field, and exposed transverse surfaces. Wen et al. [6] studied NW orientation influence on Au NW mechanical properties under tensile and compressive loading. The studied crystallographic orientations of Au NWs are [100], [110], and [111] and reported that there is a strong influence of orientations on the NW mechanical properties. Sainath et al. [7], using MD simulations studied tensile and compressive behavior of BCC Fe NWs of <100>, <110>, <111>, <112> and <102> orientations. Later Rohit et al. [8] studied the NW orientation and loading direction effect on the deformation mechanism of Cu NW. They reported that under tensile loading, all the NWs deform by twinning. Under compression, the NW of orientation <100> deform by twinning, and NW with all other orientations deform by slip. In [9], the author studied the strain rate and orientation dependence on the single-crystal titanium NW under tensile loading. The studied orientations are [11–20], [−1100], [0001] and they reported on the influence of orientation in the deformation of titanium NW at various srain rates.

In the literature, it is noticed that there are no studies on the compressive and tensile studies of NW at different orientations on a large scale. To understand the orientation influence on the tensile deformation of Ni NW in a large scale, we considered a Ni NW of dimension 100 Å × 1000 Å × 100 Å. Hence in this study, we performed the uniaxial tensile test using MD simulations on NW of four different orientations. The considered crystallographic orientation are [1–10], [20–1], [111] and [1–1–2]. The deformation mechanism and the dislocations are responsible for yield and the generated dislocation during the plastic deformation are well analyzed.

2 Simulation Details

MD simulation is used to construct and test the Ni NW of four different orientations using EAM (embedded atomic method) potential [12]. Previously, many researchers have conducted the tensile test and observed metals deformation behavior using the EAM potential. For example, Pei et al. [13] investigated Ni ductile versus brittle fracture at different temperatures. Razaei et al. [14] used the above potential in the study of Ni graphene and reported a twinning behavior. Large scale atomic/molecular massively parallel simulator (LAMMPS) [15] is used in running the MD code for studying the tensile behavior of nanocrystalline materials [5, 16–18].

The NW is created by filling a simulation box with FCC crystalline Ni atoms (a_0 = 3.518 Å) with periodic boundary conditions along the y-axis [19]. In the other two directions (x and z) non-periodic boundary conditions are applied. All the NWs have a square cross-section with a box dimension of 100 Å (x-axis) × 1000 Å (y-axis) × 100 Å (z-axis). To study the orientation effect, four highly symmetry lattice orientated Ni NWs of [1–10], [20–1], [111], and [1–1–2] are constructed as shown in Fig. 1. After the NW preparation, it is relaxed by the conjugate gradient method [19, 20] and then equilibrated at 10 K temperature using the Nose–Hoover thermostat [21]. The equilibrated NW is then deformed along the y-axis at 10^8 s^{-1} strain rate and 10 K temperature. During the tensile test, the thermodynamic ensemble NVT is used. The tensile stress is calculated by using the virial stress at a time step of 1 fs [22]. During the tensile test of NW, the defect analysis is carried by using the centrosymmetric parameter (CSP) [23] and dislocation extraction algorithm (DXA) [24] of OVITO software [25].

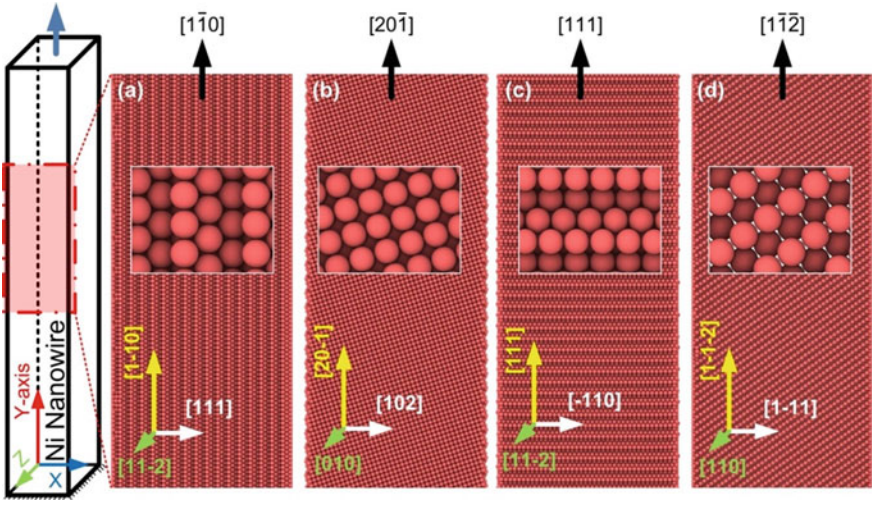

Fig. 1 Schematic view of Ni NW showing their orientations and surface structures and in the present investigation **a** [1–10], **b** [20–1], **c** [111] and **d** [1–1–2] orientations are considered

3 Results and Discussions

3.1 Stress–Strain Behavior

Figure 2 represents the true stress vs true strain curves of Ni NW of [1–10], [20–1], [111] and [1–1–2] orientations under tensile loading at 10^8 s^{-1} strain rate and 10 K temperature. All the NWs strained elastically up to yield load, followed by a sudden fall in stress. Straining the NW beyond the yield has caused plastic deformation followed by fracture at different NW regions based on their orientations. In the stress–strain curves, the slope of the initial linear region gives Young's modulus. All the mechanical properties, yield and fracture strain values are shown in Table 1. From the elastic region, it is noticed that FCC Ni NW has shown different stress–strain behavior depending on their orientation. A maximum elastic modulus of 232 GPa

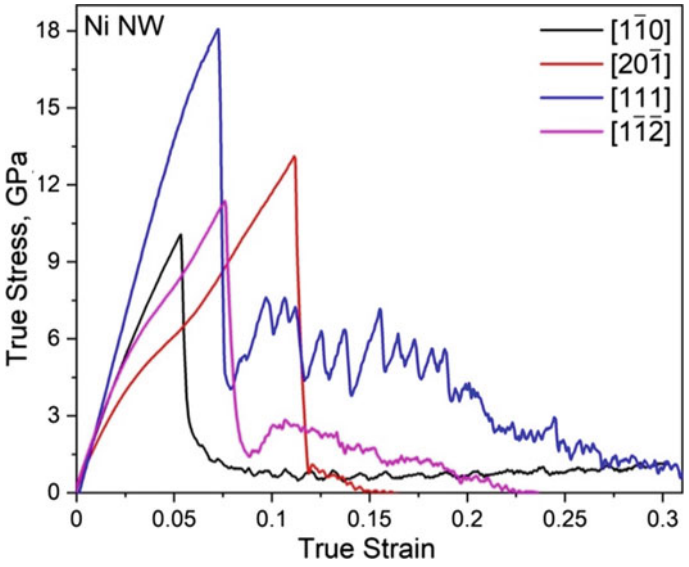

Fig. 2 True stress vs true strain curves of Ni NW of [1–10], [20–1], [111] and [1–1–2] orientations

Table 1 Mechanical properties of [1–10], [20–1], [111] and [1–1–2] Ni NW

Sl. no.	Nanowire orientation	Young's modulus GPa	Yield strength (GPa)	Yield strain	Fracture strain
1	[1–10]	172	9.5	0.053	–
2	[20–1]	90	11.7	0.112	0.152
3	[111]	232	17.2	0.075	0.352
4	[1–1–2]	120	10.5	0.076	0.225

is observed in [111] orientation followed by [1–10] (172 GPa), [1–1–2] (120 GPa) and [20–1] (90 GPa) orientations. The elastic modulus of [111] NW is more than that of nickel bulk sample ~199 GPa [26], but for [1–10] NW, it is almost close. From Fig. 2, it is noticed that the [111] orientation has recorded the highest stress ~17.2 GPa, and [1–10] orientation has the lowest stress (~9.5 GPa). The reported yield stress in [20–1] and [1–1–2] oriented NW are 11.7 and 10.5 GPa. The reported mechanical properties from the literature are based on the size, shape, temperature and at different loading conditions of NW [19, 27–29]. On a small scale, Park et al. [5] studied the tensile properties of Ni NW of <100> and <110> orientations and the reported yield stress is 8 GPa in <110> oriented NW.

3.2 Deformation Mechanisms

3.2.1 [1–10] and [20–1] oriented Ni NW

To observe the deformation mechanism during tensile loading, CSP analysis has been carried out on all NWs. In identifying the type of dislocation, we carried out DXA analysis and represented the dislocations in different colored lines. To identify the type of stacking faults, we deleted the fcc, bcc and other atoms from the sample and showed only the hcp atoms with dislocations along with stacking faults. Figure 3 represents the CSP (a) and DXA analysis (b) images at various strains during tensile loading of [1–10] (A) and [20–1] (B) oriented Ni NW. In the figure it can be observed that both the [1–10] (e = 0.053) and [20–1] (e = 0.112) NW yield by Shockley partial dislocation. The partial surrounds an intrinsic stacking fault with a burger vector of 1/6 <121>. In the process of nucleation and propagation of a Shockley partial in an FCC crystal structure, we can observe two adjacent close pack HCP atoms in-between the partials [6]. Straining the NW further, nucleation of twin partials forming twin boundaries can be observed in both [1–10] (e = 0.057) and [20–1] (e = 0.118) oriented NWs. After the yield strain (e = 0.057) the NW of [1–10] orientation has reoriented to [100] orientation due to twinning. At 14% strain, we can notice a second reorientation at the end of the [1–10] oriented NW. Straining the NW further, the twin region grows along the NW axis and hence there is an increase in the volume percentage of the reoriented region and no fracture is observed in [1–10] orientation up to 30% strain. Rohit et al. [8] have conducted tensile studies on FCC Cu NW using MD simulations and reported that there is a complete reorientation in <101>, <103>, <212>, and <214> oriented samples. In the present tensile studies, [20–1], [111] and [1–1–2] oriented NWs have been deformed up to their fracture strain but reorientation is not observed. This is due to the slip activation in more twin system which causes twin-twin interactions that results in the disruption of twin growth and reorientation [30].

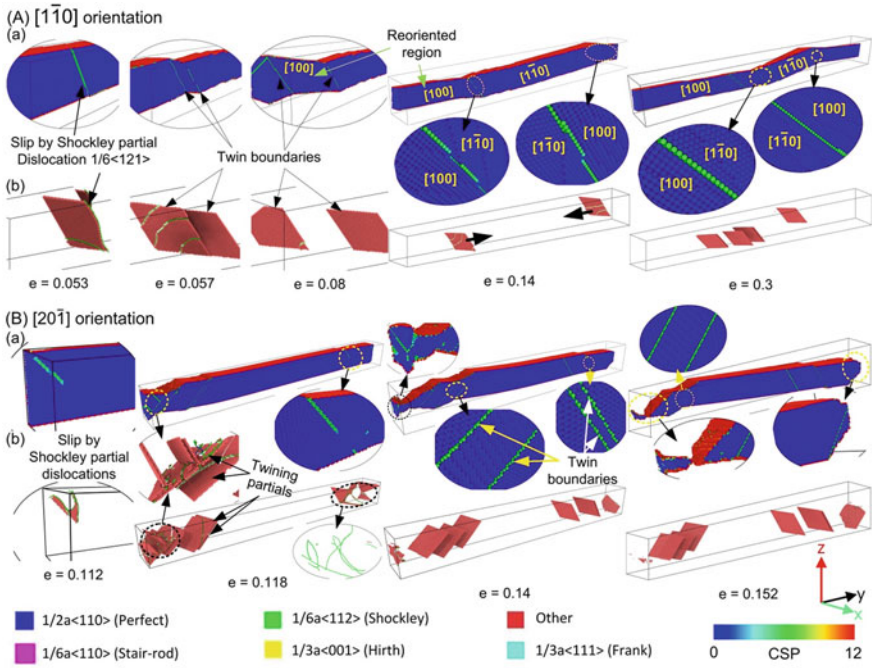

Fig. 3 Ni NW deformation behavior showing the CSP (**a**) and DXA analysis (**b**) at different strains during tensile loading in (**A**) [1–10] and (**B**) [20–1] orientations

3.2.2 [111] and [1–1–2] Oriented Ni NW

Figure 4 shows the CSP (a) and DXA analysis, (b) images at various strains during tensile loading of [111] (A) and [1–1–2] (B) oriented Ni NW. For [111] and [1–1–2] orientations, the plastic behavior is observed at the NW edge, corresponding to a strain, e = 0.075 and e = 0.076 with intrinsic stacking faults surrounded by Shockley partial dislocations. Similar deformation behavior is already shown by Zhan et al. [31] and Huang et al. [32] in their tensile deformation studies of Cu and Fe, Ni NWs using MD simulations. There is an increase in dislocation with strain in both [111] and [1–1–2] orientations after yield strain. This is because of slip activation on multiple slip systems and at strains e = 0.078 ([111]) and e = 0.08 ([1–1–2]), we can observe multiple intrinsic and extrinsic stacking faults. Dislocation densities of all oriented Ni NWs at yield strains is reported and explained in Sect. 3.3. The partials at the activated slip system start slipping on the close-packed {111} planes and their interaction results in the generation of Lomer-Cottrell (L-C) barriers [33] as shown in Fig. 4. Generally, these locks generate by the interaction of Shockley partials in different slip planes, which gives sessile stair rod dislocations as:

$$1/6\,[-21-1] + 1/6\,[1-21] \rightarrow 1/6\,[110] \tag{1}$$

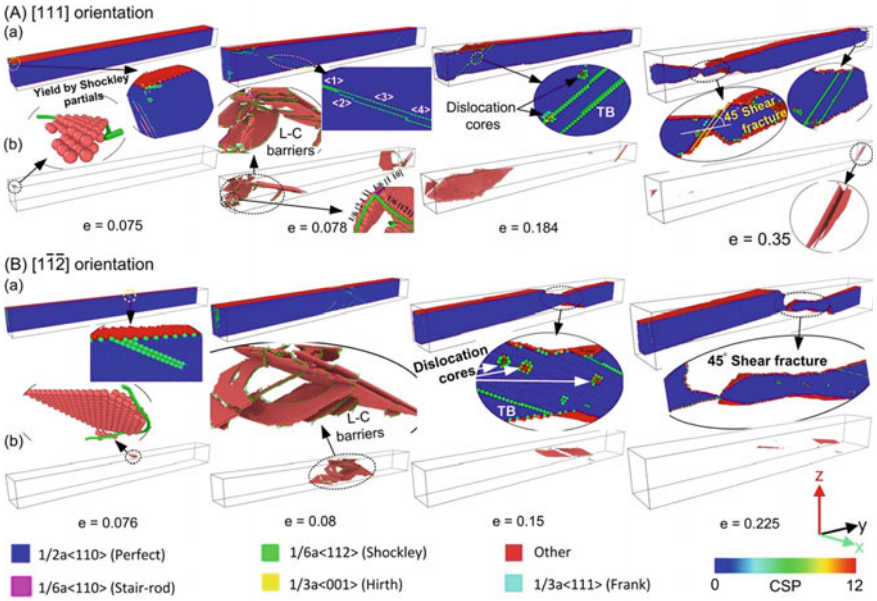

Fig. 4 Ni NW deformation behavior showing the CSP (**a**) and DXA analysis (**b**) at different strains during tensile loading in (**A**) [111] and (**B**) [1–1–2] orientations

The successive emission of partial dislocations after yield strain has transformed to a nano twin which is due to the twinning partial propagation along the initial stacking fault planes. The highlighted regions in the inset image (Fig. 4A(a) (e = 0.078)) are <1> intrinsic stacking fault; <2> extrinsic stacking fault; <3> twin formation and <4> widely separated twins. Straining the NW further, much wider twins can be observed in both [111] (e = 0.184) and [1–1–2] (e = 0.15) orientation and failed by 45° shear fracture.

3.3 Dislocation Density

Figure 5 display the dislocation densities (total and Shockley partial) of [1–10], [20–1], [111] and [1–1–2] orientated Ni NW at respective yield strains. Almost in all samples, the nucleated dislocations are Shockley partials, and they initiate the plastic deformation by slip followed by twinning. A minimum dislocation density (total) of 0.5×10^{15} m^{-2} observed in [111] and a maximum recorded in [1–10] orientation. In [34] the author studied the effect of void density on the dislocation and deformation behavior of a defective (voids) single crystal Ni of [100] orientation. The reported Shockley partial dislocation density is 50×10^{17} m^{-2} (single void), which is much higher than the present study is due to the different strain rate, orientation, sample defects, loading, and boundary conditions. In the present study dislocation density

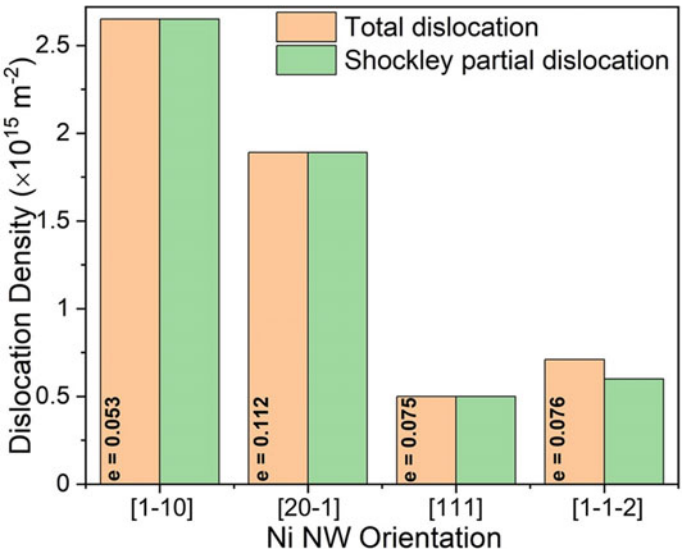

Fig. 5 Total and Shockley partial dislocation density of [1–10], [20–1], [111] and [1–1–2] oriented Ni NW at respective yield strains

increase with strain is observed in all NWs, with a significant percentage of Shockley partials.

4 Conclusions

The crystallographic orientation effect on the mechanical properties and deformation behavior of NW is studied. The tensile studies of Ni nanowires of [11–0], [20–1], [111], and [1–1–2] crystallographic orientations is carried out at 10 K temperature and deformation rate of 10^8 s^{-1}. The simulated results show that the orientation has a notable influence on NW deformation. It is noticed from the results that the NW of various orientations yields by Shockley partial dislocation with intrinsic stacking faults followed by twinning partials. The yield stress of [11–0], [20–1], [111], and [1–1–2] orientation are 9.5 GPa, 11.7 GPa, 17.2 GPa and 10.5 GPa respectively. During tensile loading, reorientation of Ni NW is noticed only in [1–10]. At yield strains, a minimum and maximum dislocation density (total) of 0.5×10^{15} m^{-2} and 2.65×10^{15} m^{-2} are observed in [111] and [1–10] oriented Ni NWs.

References

1. Peng C, Zhong Y, Lu Y, Narayanan S, Zhu T, Lou J (2013) Strain rate dependent mechanical properties in single crystal nickel nanowires. Appl Phys Lett 102:83102
2. Wang S, Shan Z, Huang H (2017) The mechanical properties of nanowires 1–24. https://doi.org/10.1002/advs.201600332
3. Sofiah AGN, Samykano M, Kadirgama K, Mohan RV, Lah NAC (2018) Metallic nanowires: mechanical properties–theory and experiment. Appl Mater Today 11:320–337. https://doi.org/10.1016/j.apmt.2018.03.004
4. Marson RL, Kuanr BK, Mishra SR, Camley RE, Celinski Z (2007) Nickel nanowires for planer microwave circuit applications and characterization. J Vac Sci Technol B Microelectron Nanom Struct 25:2619–2623. https://doi.org/10.1116/1.2801964
5. Park HS, Gall K, Zimmerman JA (2006) Deformation of FCC nanowires by twinning and slip. J Mech Phys Solids 54:1862–1881 (2006). https://doi.org/10.1016/j.jmps.2006.03.006.
6. Wen Y, Zhang Y, Wang Q, Zheng J, Zhu Z (2010) Orientation-dependent mechanical properties of Au nanowires under uniaxial loading 48:513–519. https://doi.org/10.1016/j.commatsci.2010.02.015
7. Sainath G, Choudhary BK (2016) Orientation dependent deformation behaviour of BCC iron nanowires. Comput Mater Sci 111:406–415. https://doi.org/10.1016/j.commatsci.2015.09.055
8. Rohith P, Sainath G, Choudhary BK (201) Computational condensed matter effect of orientation and mode of loading on deformation behaviour of Cu nanowires 17
9. Chang _18_Orientation and strain rate dependent tensile behavior of single crystal titanium NWs by MD.pdf, (n.d.)
10. Bin Ma_14_Effects of crystal orientation on tensile mech properties of single crystal tungsten NW.pdf, (n.d.)
11. Beretta_19_Orientation of Germanium NWs on Germanium and Silicon substrate for nanodevices.pdf, (n.d.)
12. Mendelev MI, Kramer MJ, Hao SG, Ho KM, Wang CZ (2012) Development of interatomic potentials appropriate for simulation of liquid and glass properties of nizr2 alloy. Philos Mag 92:4454–4469. https://doi.org/10.1080/14786435.2012.712220
13. Pei L, Lu C, Tieu K, Zhao X, Zhang L, Cheng K (2015) Ductile-to-brittle fracture transition in polycrystalline nickel under tensile hydrostatic stress. Comput Mater Sci 109:147–156. https://doi.org/10.1016/j.commatsci.2015.07.022
14. Rezaei R, Deng C, Tavakoli-Anbaran H, Shariati M (2016) Deformation twinning-mediated pseudoelasticity in metal–graphene nanolayered membrane. Philos Mag Lett 96:322–329. https://doi.org/10.1080/09500839.2016.1216195
15. Plimpton S (2011) LAMMPS: molecular dynamics simulator. http://lammps.sandia.gov/, Lammps. Sandia. Gov
16. Ruan Z, Wu W, Li N (2018) Effects of strain rate, temperature and grain size on the mechanical properties and microstructure evolutions of polycrystalline nickel nanowires: a molecular dynamics simulation. Wuhan Univ J Nat Sci 23:251–258. https://doi.org/10.1007/s11859-018-1318-x
17. Monk J, Farkas D (2007) Tension-compression asymmetry and size effects in nanocrystalline Ni nanowires. Philos Mag 87:2233–2244. https://doi.org/10.1080/14786430701361404
18. Zhang T, Zhou K, Chen ZQ (2015) Strain rate effect on plastic deformation of nanocrystalline copper investigated by molecular dynamics. Mater Sci Eng A 648:23–30. https://doi.org/10.1016/j.msea.2015.09.035
19. Wen YH, Zhu ZZ, Zhu RZ (2008) Molecular dynamics study of the mechanical behavior of nickel nanowire: Strain rate effects. Comput Mater Sci 41:553–560. https://doi.org/10.1016/j.commatsci.2007.05.012
20. Liu Y, Zhao J (2011) The size dependence of the mechanical properties and breaking behavior of metallic nanowires: a statistical description. Comput Mater Sci 50:1418–1424. https://doi.org/10.1016/j.commatsci.2010.11.026

21. Hoover WG (1985) Canonical dynamics: equilibrium phase-space distributions. Phys Rev A
22. Diao J, Gall K, Dunn ML, Zimmerman JA (2006) Atomistic simulations of the yielding of gold nanowires. Acta Mater 54:643–653. https://doi.org/10.1016/j.actamat.2005.10.008
23. Kelchner CL, Plimpton SJ, Hamilton JC (1998) Dislocation nucleation and defect structure during surface indentation. Phys Rev B 58:11085
24. Stukowski A, Bulatov VV, Arsenlis A (2012) Automated identification and indexing of dislocations in crystal interfaces. Model Simul Mater Sci Eng 20. https://doi.org/10.1088/0965-0393/20/8/085007
25. Stukowski A (2010) Visualization and analysis of atomistic simulation data with OVITO-the open visualization tool. Model Simul Mater Sci Eng 18. https://doi.org/10.1088/0965-0393/18/1/015012
26. Hertzberg RW (1983) Deformation and fracture mechanics of engineering materials. Wiley 1983:697
27. Setoodeh AR, Attariani H, Khosrownejad M (2008) Nickel nanowires under uniaxial loads: a molecular dynamics simulation study. Comput Mater Sci 44:378–384. https://doi.org/10.1016/j.commatsci.2008.03.035
28. Wen YH, Zhu ZZ, Shao GF, Zhu RZ (2005) The uniaxial tensile deformation of Ni nanowire: atomic-scale computer simulations. Phys E Low-Dimensional Syst Nanostruct 27:113–120. https://doi.org/10.1016/j.physe.2004.10.009
29. Wang WD, Yi CL, Fan KQ (2013) Molecular dynamics study on temperature and strain rate dependences of mechanical tensile properties of ultrathin nickel nanowires. Trans Nonferrous Met Soc China 23: 3353–3361. https://doi.org/10.1016/S1003-6326(13)62875-7
30. Sainath G, Choudhary BK, Jayakumar T (2015) Molecular dynamics simulation studies on the size dependent tensile deformation and fracture behaviour of body centred cubic iron nanowires. Comput Mater Sci 104:76–83. https://doi.org/10.1016/j.commatsci.2015.03.053
31. Zhan HF, Gu YT, Yan C, Feng XQ, Yarlagadda PKDV (2011) Numerical exploration of plastic deformation mechanisms of copper nanowires with surface defects. Comput Mater Sci 50:3425–3430. https://doi.org/10.1016/j.commatsci.2011.07.004
32. Huang D, Zhang Q, Guo Y (2006) Molecular dynamics simulation for axial tension process of α-Fe and Ni nano wires. Ordnance Mater Sci Eng 5:4
33. Zhang Y, Jiang S, Zhu X, Zhao Y (2016) A molecular dynamics study of intercrystalline crack propagation in nano-nickel bicrystal films with (0 1 0) twist boundary. Eng Fract Mech 168:147–159. https://doi.org/10.1016/j.engfracmech.2016.10.008
34. Yanqiu Zhang YZ, Jiang S, Zhu X (2017) Influence of void density on dislocation mechanisms of void shrinkage in nickel single crystal based on molecular dynamics simulation. Phys E 90:90–97